

Sea urchin sperm exploit extremum seeking control to find the egg

Mahmoud Abdelgalil^{1,*}, Yasser Aboelkassem^{2,3}, Haithem Taha¹

¹ Mechanical and Aerospace Engineering Department, University of California at Irvine, Irvine, CA 92697

² College of Innovation and Technology, University of Michigan at Flint, Flint MI 48502

³ Michigan Institute for Data Science, University of Michigan, Ann Arbor MI 48109

Abstract

Sperm perform extremely demanding tasks with minimal mechanosensory capabilities. The cells must quickly navigate in a noisy environment and find an egg within a short time window for successful fertilization without any global positioning information. Many research efforts have been dedicated to derive mathematical principles that explain their superb navigation strategy. Here we discover that the navigation strategy of sea urchin sperm is a well-established adaptive control technique known as extremum seeking. This bridge between mathematical control theory and the biology of taxis in microorganisms is expected to deepen our understanding of the process. For example, it suggests the characterization of the signaling pathway as an adaptive band pass filter. Moreover, it will guide engineers in developing bio-inspired miniaturized robots for source seeking with minimal sensors.

Introduction

Source seeking is the problem of locating an object that emits a scalar signal (e.g. temperature, light intensity, or chemical concentration), typically without global positioning information [12]. Many living organisms are routinely faced with the source seeking problem. A well studied example is that of sperm chemotaxis in sea urchins. To locate an egg in open water, sea urchin sperm evolved to swim up the gradient of the concentration field established by the diffusion of a chemoattractant sperm-activating peptide (SAP) released by sea urchin eggs [2]. Notably, the navigation strategy of sea urchin sperm is deterministic; the cells employ the mean curvature of the flagellum controlled by intracellular calcium as a steering feedback mechanism to swim in circular paths that drift in the direction of the gradient in 2D, and in helical paths that align with the gradient in 3D [4, 6, 9]. This feedback mechanism is mediated by a complex signaling pathway that regulates the influx and efflux of calcium in the cell [10, 14]. We bridge a gap between mathematical control theory and the taxis of microorganisms by framing the search for the egg as a source seeking problem and demonstrating that the navigation strategy of sea urchin sperm is in fact a natural implementation of a well established adaptive control paradigm known as extremum seeking [12, 15].

The hallmarks of an extremum seeking solution to the source seeking problem are: i) injection of periodic perturbation signals to sample the local signal strength, ii) a filter that measures the instantaneous signal strength and extracts the oscillations due to the perturbation signals, iii) demodulation of the local gradient information from the filter's output, and iv) an integrator that

biases the motion in the direction of the gradient [13]. We show that the kinematics of the swimming pattern naturally provide the roles of the periodic perturbation, demodulation, and integration components of the standard extremum seeking loop (Fig. 1). The characterization of sea urchin sperm chemotaxis as an extremum seeking problem suggests modeling the signaling pathway as an adaptive band pass filter. In this manner, the swimming kinematics of sea urchin sperm, together with the signaling pathway, naturally constitute an extremum seeking strategy for chemotaxis.

Modeling the sperm motion

Swimming in the low Reynolds number fluid regime is dominated by viscous forces, which enables the use of kinematic models as good approximations to the motion of micro-swimmers, including sperm cells [7]. The kinematics of a rigid body is:

$$\dot{\mathbf{p}}(t) = \mathbf{R}(t)\mathbf{V}, \quad \dot{\mathbf{R}}(t) = \mathbf{R}(t)\widehat{\boldsymbol{\Omega}} \quad (1)$$

where the vectors \mathbf{V} and $\boldsymbol{\Omega}$ are the linear and angular velocity vectors as represented in the body frame, $\widehat{\boldsymbol{\Omega}}$ denotes the skew-symmetric matrix corresponding to the angular velocity vector $\boldsymbol{\Omega}$, $\mathbf{p}(t)$ is the instantaneous position of the body with respect to the origin of a fixed frame of reference, and $\mathbf{R}(t)$ is the instantaneous rotation matrix that relates the body frame to the fixed frame. In the case of sea urchin sperm, the mean curvature and torsion of the flagellar beating pattern, which are regulated by the chemotactic signaling pathway, control the angular velocities in the body frame [2]. A common model of the effect of the chemotactic signaling pathway on the swimming kinematics of sea urchin sperm is given by the relations:

$$\mathbf{V} = [v \ 0 \ 0]^\top, \quad \boldsymbol{\Omega} = [\omega_{\parallel}(t) \ 0 \ \omega_{\perp}(t)]^\top \quad (2)$$

where $v > 0$ is constant, and the angular velocity components $\omega_{\parallel}(t)$ and $\omega_{\perp}(t)$ are given by:

$$\omega_{\parallel}(t) = \omega_{\parallel,0} + \omega_{\parallel,1}\eta(t), \quad \omega_{\perp}(t) = \omega_{\perp,0} + \omega_{\perp,1}\eta(t), \quad (3)$$

with $\omega_{\perp,0}, \omega_{\perp,1}, \omega_{\parallel,0}, \omega_{\parallel,1}$ as constant coefficients, and $\eta(\cdot)$ as a dynamic feedback term regulated by the signaling pathway [5, 6, 9].

An extremum seeking loop

The constant angular velocity components $\omega_{\parallel,0}$ and $\omega_{\perp,0}$ lead to a periodic swimming pattern which injects periodic perturbations with zero average into the position and orientation of the cell. To study the average motion of the cell, we remove these periodic variations from the motion by defining the constant angular velocity vector $\boldsymbol{\Omega}_0$:

$$\boldsymbol{\Omega}_0 = [\omega_{\parallel,0} \ 0 \ \omega_{\perp,0}]^\top \quad (4)$$

and the average position and orientation as:

$$\bar{\mathbf{p}}(t) = \mathbf{p}(t) - \varepsilon \bar{\mathbf{R}}(t)\boldsymbol{\delta}(\omega t), \quad \bar{\mathbf{R}}(t) = \mathbf{R}(t) \exp(\widehat{\boldsymbol{\Omega}}_0 t)^\top \quad (5)$$

whose dynamics can be exactly written as:

$$\dot{\bar{\mathbf{p}}}(t) = \bar{\mathbf{R}}(t)\mathbf{V}_{\eta}(\omega t)\eta(t)\varepsilon + \bar{\mathbf{R}}(t)\bar{\mathbf{V}} \quad (6)$$

$$\dot{\bar{\mathbf{R}}}(t) = \bar{\mathbf{R}}(t)\widehat{\boldsymbol{\Omega}}_{\eta}(\omega t)\eta(t) \quad (7)$$

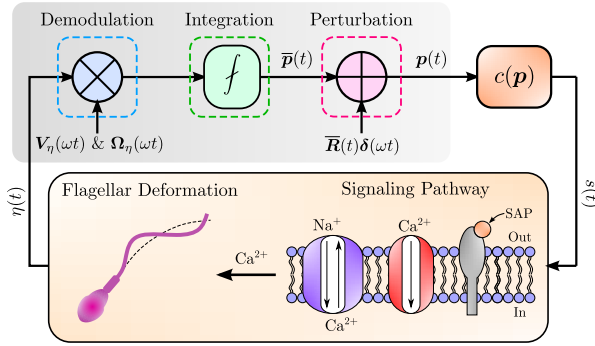


Figure 1: **Block diagram description of sperm chemotaxis.** The swimming pattern injects periodic perturbations into the instantaneous position of the cell which leads to oscillations in the stimulus. The signaling pathway relays these periodic perturbations to the angular velocities through flagellar deformation. Then, the periodic feedback coefficients (i.e. \mathbf{V}_η and $\mathbf{\Omega}_\eta$) of the dynamics of average motion demodulate the gradient information carried by the feedback signal $\eta(t)$ through signal multiplication. Finally, the kinematic integrator biases the motion in the direction of the gradient. Most hallmarks (i.e. periodic perturbation, demodulation, and integration) of extremum seeking are apparent in this feedback loop. As such, the extremum seeking formulation suggests that the filtration role is played by the signaling pathway.

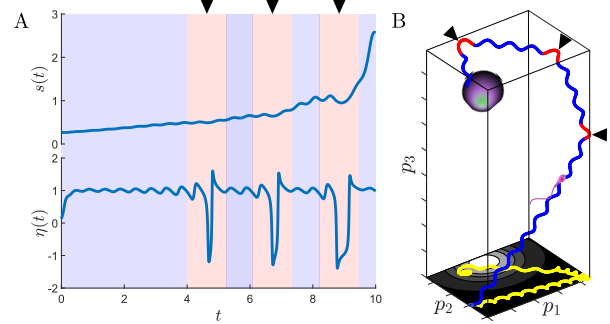


Figure 2: **Sample response and trajectory in a radial concentration field.** The simulation parameters are: $v = l_0 \text{ sec}^{-1}$, $\omega_{\perp,0} = -7 \text{ sec}^{-1}$, $\omega_{\parallel,0} = -5 \text{ sec}^{-1}$, $\sigma_1 = 2\omega^{-1}$, $\sigma_2 = \omega^{-1}$, $\mu = \omega^{-1}/3$, $\omega_{\perp,1} = -1$, $\omega_{\parallel,1} = -5$, l_0 is a characteristic length, and the concentration field is $c(\mathbf{p}) = l_0 \|\mathbf{p}\|^{-1}$. The initial conditions are: $\mathbf{p}(0) = -(l_0, l_0, 3.5l_0)$, $\mathbf{R}(0)$ is the identity matrix, $\zeta_1(0) = 0.75c(\mathbf{p}(0))$, $\zeta_2(0) = 1.25c(\mathbf{p}(0))$, $\rho(0) = 1$. When $l_0 = 200 \mu\text{m}$, the velocities v , $\omega_{\perp,0}$ and $\omega_{\parallel,0}$ agree with their experimentally observed values [5]. **A:** the stimulus signal $s(t) = c(\mathbf{p}(t))$ and the feedback signal $\eta(t)$ where black arrows indicate the intervals when the stimulus is not increasing and high amplitude steering response, **B:** the spatial trajectory of the cell $\mathbf{p}(t)$ where the black arrows indicate the segments of the trajectory where a strong deformation takes place.

where $\omega = (\omega_{\perp,0}^2 + \omega_{\parallel,0}^2)^{\frac{1}{2}}$ is the temporal frequency of the periodic swimming pattern, $\varepsilon = 1/\omega$, the vector $\bar{\mathbf{V}}$ is the average velocity vector represented in body coordinates without any feedback from the signaling pathway, the vector $\delta(\omega t)$ is the periodic perturbation in the position injected by the swimming pattern, and the vectors $\mathbf{V}_\eta(\omega t)$ and $\mathbf{\Omega}_\eta(\omega t)$ are the feedback coefficients of the average kinematics (see the SI appendix for exact expressions). The periodic perturbation $\delta(\omega t)$ has zero average, whereas the coefficients $\mathbf{V}_\eta(\omega t)$ and $\mathbf{\Omega}_\eta(\omega t)$ are periodic with non zero average.

Fig. 1 provides a block diagram description of the dynamical equations [5]-[7] representing the navigation strategy of sea urchin sperm, where $c(\mathbf{p})$ is the SAP concentration at the point \mathbf{p} and the special integration symbol f denotes the nonholonomic kinematic integrator defined by equations [6] and [7]. The block diagram reveals a vivid connection between sperm chemotaxis and extremum seeking. In this diagram, most components (i.e. perturbation, demodulation and integration) of extremum seeking are clearly present. An immediate outcome of the proposed connection between sperm chemotaxis and extremum seeking is the realization that the signaling pathway must be playing the role of filtration.

Chemotactic sensing

Having established the connection between the chemotactic navigation strategy of sea urchin sperm and extremum seeking, which suggests the characterization of the dynamics of the signaling pathway as a band pass filter, it is interesting to connect such dynamics to the intracellular processes involved in sea urchin sperm chemotaxis. Experiments show that a step increase in the SAP concentration initiates rapid synthesis of cGMP in the cell which triggers a cascade of cellular events leading to the influx of calcium by opening calcium permeable channels (stimulation). Hydrolysis of cGMP and the efflux of calcium relax the response to resting levels [2] (relaxation). We model the response of the signaling pathway by the difference between stimulation and relaxation as in the following system of differential equations:

$$\sigma_1 \dot{\zeta}_1(t) = \zeta_2(t) - \zeta_1(t), \quad \sigma_2 \dot{\zeta}_2(t) = s(t) - \zeta_2(t) \quad (8)$$

$$\zeta(t) = \zeta_2(t) - \zeta_1(t) \quad (9)$$

$$\mu \dot{\rho}(t) = \rho(t) (1 - (\rho(t)\zeta(t))^2), \quad \eta(t) = \rho(t)\zeta(t) \quad (10)$$

where μ, σ_1, σ_2 are positive constants, and $\sigma_2 \leq \sigma_1$. We note that the signals $\zeta_2(t)$ and $\zeta_1(t)$ model the stimulation and relaxation processes, respectively. It is clear that equations [8]-[9] represent a band pass filter. Equation [10] models the adaptation of the signaling pathway. During the course of motion, the cell is exposed to a time varying stimulus $s(t) = c(\mathbf{p}(t))$ through the binding of SAP molecules with receptors along the flagellum [2]. This stimulus may be approximated by its Taylor series over an $\mathcal{O}(\varepsilon)$ time duration $t_0 \leq t \leq t_0 + \varepsilon$ (relying on the relations [5] and [6]):

$$s(t) \approx s(t_0) + \varepsilon \nabla c(\bar{\mathbf{p}}(t_0))^\top \bar{\mathbf{R}}(t_0) (\bar{\mathbf{V}}\omega\Delta t + \boldsymbol{\delta}(\omega t)) \quad (11)$$

where $\Delta t = t - t_0$. The gradient information is modulated in the stimulus on two components: a ramp component and a harmonic component. One can simply extract the gradient information from the stimulus by time differentiation. However, a simple differentiator is notoriously known for high frequency noise amplification leading to deteriorated performance in the case of noise-corrupted signals which is the typical case in chemotaxis [8]. Hence, a band pass filter whose quasi steady state carries the gradient information is more robust in the presence of noise.

Applying the stimulus $s(t)$ as in equation [11] to the model of the signaling pathway given by equations [8]-[10] leads to a response whose quasi-steady output $\eta(t)$ can be approximated by:

$$\eta(t) \approx (\rho_1 \bar{\mathbf{V}} + \rho_2 \boldsymbol{\delta}(\omega t + \phi))^\top \bar{\mathbf{R}}(t) \frac{\nabla c(\bar{\mathbf{p}}(t))}{\|\nabla c(\bar{\mathbf{p}}(t))\|} \quad (12)$$

where ρ_1 and ρ_2 are non negative gain functions that are independent from the magnitude of the gradient, and ϕ is the phase lag introduced by the dynamics of the signaling pathway (see the SI appendix for exact expressions). Closing the feedback loop with equation [12] into the average kinematics of sperm motion (i.e. equations [6] and [7]) modifies the net motion of the cell via two mechanisms: i) the change in the orientation due to $\boldsymbol{\Omega}_\eta(\omega t)\eta(t)$, and ii) the bias in the direction of motion due to $\mathbf{V}_\eta(\omega t)\eta(t)$. A standard averaging analysis in the fast time variable $\sigma = \omega t$ may be used to study the average motion of the cell under this feedback (see the SI appendix for more details). Fig. 2 shows a sample response of the system defined by [1]-[3] under the feedback law defined by [8]-[10].

When the motion is confined to the plane (i.e. when $\omega_{\parallel,0} = \omega_{\parallel,1} = 0$), the averaging analysis yields the following differential equation for the average position $\bar{\mathbf{p}}(t)$:

$$\frac{d}{dt} (c(\bar{\mathbf{p}}(t))) = -\gamma \omega_{\perp,0} \omega_{\perp,1} \sin(\phi) \|\nabla c(\bar{\mathbf{p}}(t))\|, \quad (13)$$

where γ is a positive constant, which is a gradient based strategy. That is, the periodic swimming pattern of the sperm, along with the tuned band-pass filter dynamics of the signaling pathway, manage to guide the average motion of the sperm in the direction of the gradient without direct access to any gradient information, which is the typical task of any extremum seeking algorithm. It should be noted that the dynamics in equation [13] is a gradient ascent only if $\omega_{\perp,0} \omega_{\perp,1} \sin(\phi) < 0$, which is interestingly deduced in [6] from a different perspective. The details for the 3D case are more intricate due to the nonholonomic nature of the kinematic integrator defined by equations [6] and [7]. Thus, we include the averaging analysis and its results for the 3D case in the SI appendix. Remarkably, similar versions of the navigation strategy presented here have been independently proposed as extremum seeking algorithms for nonholonomic vehicles [3,15]; the current paper establishes a natural connection between these algorithms and sperm chemotaxis.

Discussion

Helical klinotaxis is a ubiquitous mode of taxis in microorganisms including sperm cells [4]. In this manuscript, we established a connection between helical klinotaxis and the adaptive control paradigm known as extremum seeking. This connection sheds light on the role played by the chemotactic signaling pathway in sea urchin sperm and suggests the characterization of its dynamics as an adaptive band pass filter. The signaling pathway involved in the chemotaxis of sea urchin sperm is complex [14], and the binding of the SAP molecules with receptors is a noisy process [11]. However, it is remarkable that the observed response of the signaling pathway in sea urchin sperm exhibits the essential features of the response of a band pass filter [1,10]. Moreover, our analysis and simulations show that when the average direction of motion is aligned with the gradient and the average stimulus is increasing, the periodic component in the response $\eta(t)$ of the signaling pathway model is attenuated (the blue intervals in Fig. 2A), resulting in only slight adjustment of the direction of average motion (the blue segments in Fig. 2B). On the other hand, when the average direction of motion is mostly orthogonal to the gradient and the average stimulus is non increasing, the periodic component is amplified (the red intervals in Fig. 2A), resulting in a vigorous adjustment of the trajectory (the red segments in Fig. 2B). As such, the suggested characterization of the signaling pathway as an adaptive band pass filter naturally reproduces the experimentally observed switching behavior between low gain and high gain steering modes, also known as the “on” and “off” responses, in sea urchin sperm 3D chemotaxis [9,11].

It is intriguing that all these observations of the behavior of the signaling pathway corroborate its characterization as an adaptive band-pass filter — an immediate implication of the proposed extremum seeking formulation of the navigation strategy of sea urchin sperm.

References

- [1] Luis Alvarez, Luru Dai, Benjamin M Friedrich, Nachiket D Kashikar, Ingo Gregor, René Pascal, and U Benjamin Kaupp. The rate of change in ca2+ concentration controls sperm chemotaxis. *Journal of Cell Biology*, 196(5):653–663, 2012.
- [2] Luis Alvarez, Benjamin M Friedrich, Gerhard Gompper, and U Benjamin Kaupp. The computational sperm cell. *Trends in cell biology*, 24(3):198–207, 2014.

-
- [3] Jennie Cochran, Antranik Siranosian, Nima Ghods, and Miroslav Krstic. 3-d source seeking for underactuated vehicles without position measurement. *IEEE Transactions on Robotics*, 25(1):117–129, 2009.
- [4] Hugh C Crenshaw. Orientation by helical motion—iii. microorganisms can orient to stimuli by changing the direction of their rotational velocity. *Bulletin of Mathematical Biology*, 55(1):231–255, 1993.
- [5] Hugh C Crenshaw. A new look at locomotion in microorganisms: rotating and translating. *American Zoologist*, 36(6):608–618, 1996.
- [6] Benjamin M Friedrich and Frank Jülicher. Chemotaxis of sperm cells. *Proceedings of the National Academy of Sciences*, 104(33):13256–13261, 2007.
- [7] Benjamin M Friedrich, Ingmar H Riedel-Kruse, Jonathon Howard, and Frank Jülicher. High-precision tracking of sperm swimming fine structure provides strong test of resistive force theory. *Journal of Experimental Biology*, 213(8):1226–1234, 2010.
- [8] BM Friedrich and F Jülicher. The stochastic dance of circling sperm cells: sperm chemotaxis in the plane. *New Journal of Physics*, 10(12):123025, 2008.
- [9] Jan F Jikeli, Luis Alvarez, Benjamin M Friedrich, Laurence G Wilson, René Pascal, Remy Colin, Magdalena Pichlo, Andreas Rennhack, Christoph Brenker, and U Benjamin Kaupp. Sperm navigation along helical paths in 3d chemoattractant landscapes. *Nature communications*, 6(1):1–10, 2015.
- [10] U Benjamin Kaupp, Johannes Solzin, Eilo Hildebrand, Joel E Brown, Annika Helbig, Volker Hagen, Michael Beyermann, Francesco Pampaloni, and Ingo Weyand. The signal flow and motor response controlling chemotaxis of sea urchin sperm. *Nature cell biology*, 5(2):109–117, 2003.
- [11] Justus A Kromer, Steffen Märcker, Steffen Lange, Christel Baier, and Benjamin M Friedrich. Decision making improves sperm chemotaxis in the presence of noise. *PLoS computational biology*, 14(4):e1006109, 2018.
- [12] Miroslav Krstic and Jennie Cochran. Extremum seeking for motion optimization: From bacteria to nonholonomic vehicles. In *2008 Chinese Control and Decision Conference*, pages 18–27. IEEE, 2008.
- [13] Miroslav Krstic and Hsin-Hsiung Wang. Stability of extremum seeking feedback for general nonlinear dynamic systems. *Automatica-Kidlington*, 36(4):595–602, 2000.
- [14] Daniel A Priego-Espinosa, Alberto Darszon, Adán Guerrero, Ana Laura González-Cota, Takuya Nishigaki, Gustavo Martínez-Mekler, and Jorge Carneiro. Modular analysis of the control of flagellar ca^{2+} -spike trains produced by catsper and cav channels in sea urchin sperm. *PLoS computational biology*, 16(3):e1007605, 2020.
- [15] Alexander Scheinker and Miroslav Krstić. Extremum seeking with bounded update rates. *Systems & Control Letters*, 63:25–31, 2014.

1 Supporting Information Text

If the angular velocity components $\omega_{\perp}(\cdot)$ and $\omega_{\parallel}(\cdot)$ are given by:

$$\omega_{\perp}(t) = \omega_{\perp,0} + \omega_{\perp,1}\eta(t), \quad [1]$$

$$\omega_{\parallel}(t) = \omega_{\parallel,0} + \omega_{\parallel,1}\eta(t), \quad [2]$$

then we may rewrite the rotational kinematics as:

$$\dot{\mathbf{R}}(t) = \mathbf{R}(t) \left(\widehat{\boldsymbol{\Omega}}_0 + \widehat{\boldsymbol{\Omega}}_1 \eta(t) \right) \quad [3]$$

where the vectors $\boldsymbol{\Omega}_0$ and $\boldsymbol{\Omega}_1$ are given by:

$$\boldsymbol{\Omega}_0 = \begin{bmatrix} \omega_{\parallel,0} \\ 0 \\ \omega_{\perp,0} \end{bmatrix}, \quad \boldsymbol{\Omega}_1 = \begin{bmatrix} \omega_{\parallel,1} \\ 0 \\ \omega_{\perp,1} \end{bmatrix} \quad [4]$$

Let $\mathbf{R}_0(t) = \exp(\widehat{\boldsymbol{\Omega}}_0 t)$ and $\overline{\mathbf{R}}(t) = \mathbf{R}(t)\mathbf{R}_0(t)^\top$, and compute:

$$\mathbf{R}_0(t) = \begin{pmatrix} \frac{\omega_{\perp,0}^2}{\omega^2} \cos(\omega t) + \frac{\omega_{\parallel,0}^2}{\omega^2} & -\frac{\omega_{\perp,0}}{\omega} \sin(\omega t) & \frac{\omega_{\perp,0}\omega_{\parallel,0}}{\omega^2} (1 - \cos(\omega t)) \\ \frac{\omega_{\perp,0}}{\omega} \sin(\omega t) & \cos(\omega t) & -\frac{\omega_{\parallel,0}}{\omega} \sin(\omega t) \\ \frac{\omega_{\perp,0}\omega_{\parallel,0}}{\omega^2} (1 - \cos(\omega t)) & \frac{\omega_{\parallel,0}}{\omega} \sin(\omega t) & \frac{\omega_{\parallel,0}^2}{\omega^2} \cos(\omega t) + \frac{\omega_{\perp,0}^2}{\omega^2} \end{pmatrix} \quad [5]$$

Then, observe that:

$$\begin{aligned} \dot{\mathbf{p}}(t) &= \mathbf{R}(t)\mathbf{V} = \mathbf{R}(t)\mathbf{R}_0(t)^\top \mathbf{R}_0(t)\mathbf{V} = \overline{\mathbf{R}}(t)\mathbf{R}_0(t)\mathbf{V} \\ \dot{\overline{\mathbf{R}}}(t) &= \dot{\mathbf{R}}(t)\mathbf{R}_0(t)^\top + \mathbf{R}(t)\dot{\mathbf{R}}_0(t)^\top = \mathbf{R}(t)\widehat{\boldsymbol{\Omega}}_0\mathbf{R}_0(t)^\top + \eta(t)\mathbf{R}(t)\widehat{\boldsymbol{\Omega}}_1\mathbf{R}_0(t)^\top - \mathbf{R}(t)\widehat{\boldsymbol{\Omega}}_0\mathbf{R}_0(t)^\top \\ &= \mathbf{R}(t)\mathbf{R}_0(t)^\top \mathbf{R}_0(t)\widehat{\boldsymbol{\Omega}}_1\mathbf{R}_0(t)^\top \eta(t) \end{aligned}$$

where $\omega = \sqrt{\omega_{\perp,0}^2 + \omega_{\parallel,0}^2}$. Let $v > 0$, $|\omega_{\perp,0}| > 0$, and :

$$\mathbf{e}_1 = \begin{pmatrix} \frac{\omega_{\parallel,0}}{\omega} \\ 0 \\ \frac{\omega_{\perp,0}}{\omega} \end{pmatrix}, \quad \mathbf{e}_3(\omega t) = \begin{pmatrix} \frac{\omega_{\perp,0}}{\omega} \cos(\omega t) \\ \sin(\omega t) \\ -\frac{\omega_{\parallel,0}}{\omega} \cos(\omega t) \end{pmatrix} \quad [6]$$

then observe that $\|\mathbf{e}_1\| = \|\mathbf{e}_3(\cdot)\| = 1$, and that:

$$\mathbf{R}_0(t)\mathbf{V} = \frac{v\omega_{\parallel,0}}{\omega} \mathbf{e}_1 + \frac{v\omega_{\perp,0}}{\omega} \mathbf{e}_3(\omega t) \quad [7]$$

$$\mathbf{R}_0(t)\widehat{\boldsymbol{\Omega}}_1\mathbf{R}_0(t)^\top = \left(\omega_{\perp,1} \frac{\omega_{\perp,0}}{\omega} + \omega_{\parallel,1} \frac{\omega_{\parallel,0}}{\omega} \right) \widehat{\mathbf{V}}_1 + \left(\omega_{\parallel,1} \frac{\omega_{\perp,0}}{\omega} - \frac{\omega_{\parallel,0}}{\omega} \omega_{\perp,1} \right) \widehat{\mathbf{V}}_3(\omega t) \quad [8]$$

Consequently, we have that:

$$\dot{\mathbf{p}}(t) = \overline{\mathbf{R}}(t) \left(\frac{v\omega_{\perp,0}}{\omega} \mathbf{e}_3(\omega t) + \frac{v\omega_{\parallel,0}}{\omega} \mathbf{e}_1 \right) \quad [9]$$

If we integrate both sides with respect to t , we obtain:

$$\mathbf{p}(\sigma)|_0^t = \frac{v\omega_{\perp,0}}{\omega} \int_0^t \overline{\mathbf{R}}(\sigma) \mathbf{e}_3(\omega\sigma) d\sigma + \frac{v\omega_{\parallel,0}}{\omega} \int_0^t \overline{\mathbf{R}}(\sigma) \mathbf{e}_1 d\sigma \quad [10]$$

Integrating the first term on the right hand side by parts yields:

$$\mathbf{p}(s)|_0^t = \frac{v\omega_{\perp,0}}{\omega^2} \overline{\mathbf{R}}(\sigma) \mathbf{e}_2(\omega\sigma)|_0^t - \frac{v\omega_{\perp,0}}{\omega^2} \int_0^t \overline{\mathbf{R}}(\sigma) \mathbf{R}_0(\sigma) \widehat{\boldsymbol{\Omega}}_1 \mathbf{R}_0(\sigma)^\top \mathbf{e}_2(\omega\sigma) \eta(\sigma) d\sigma + \frac{v\omega_{\parallel,0}}{\omega} \int_0^t \overline{\mathbf{R}}(\sigma) \mathbf{e}_1 d\sigma \quad [11]$$

where

$$\mathbf{e}_2(\omega\sigma) = \int \mathbf{e}_3(\omega\sigma) d(\omega\sigma) = \begin{pmatrix} \frac{\omega_{\perp,0}}{\omega} \sin(\omega\sigma) \\ -\cos(\omega\sigma) \\ -\frac{\omega_{\parallel,0}}{\omega} \sin(\omega\sigma) \end{pmatrix} \quad [12]$$

Observe that $\mathbf{e}_2(\cdot)$ is periodic with zero average, $\|\mathbf{e}_2(\cdot)\|=1$, and that:

$$\mathbf{e}_1 \times \mathbf{e}_2(\omega t) = \mathbf{e}_3(\omega t) \quad [13]$$

$$\mathbf{e}_2(\omega t) \times \mathbf{e}_3(\omega t) = \mathbf{e}_1 \quad [14]$$

$$\mathbf{e}_3(\omega t) \times \mathbf{e}_1 = \mathbf{e}_2(\omega t) \quad [15]$$

$$\mathbf{e}_2(\omega t + \phi_0) = \cos(\phi_0)\mathbf{e}_2(\omega t) + \sin(\phi_0)\mathbf{e}_3(\omega t) \quad [16]$$

where \times denotes the cross product between 3D vectors. Move the first term on the right hand side in Eq 11 to the left hand side and differentiate both sides again to obtain:

$$\frac{d}{dt} \left(\mathbf{p}(t) - \frac{v\omega_{\perp,0}}{\omega^2} \overline{\mathbf{R}}(t) \mathbf{e}_2(\omega t) \right) = \overline{\mathbf{R}}(t) \left(-\frac{v\omega_{\perp,0}}{\omega^2} \mathbf{R}_0(t) \widehat{\boldsymbol{\Omega}}_1 \mathbf{R}_0(t)^\top \mathbf{e}_2(\omega t) \eta(t) + \frac{v\omega_{\parallel,0}}{\omega} \mathbf{e}_1 \right) \quad [17]$$

If we make the identifications:

$$\boldsymbol{\delta}(\omega t) = \frac{v\omega_{\perp,0}}{\omega} \mathbf{e}_2(\omega t) \quad [18]$$

$$\overline{\mathbf{V}} = \frac{v\omega_{\parallel,0}}{\omega} \mathbf{e}_1 \quad [19]$$

$$\overline{\mathbf{p}}(t) = \mathbf{p}(t) - \frac{1}{\omega} \overline{\mathbf{R}}(t) \boldsymbol{\delta}(\omega t) \quad [20]$$

$$\widehat{\boldsymbol{\Omega}}_\eta(\omega t) = \mathbf{R}_0(t) \widehat{\boldsymbol{\Omega}}_1 \mathbf{R}_0(t)^\top \quad [21]$$

$$\mathbf{V}_\eta(\omega t) = -\widehat{\boldsymbol{\Omega}}_\eta(\omega t) \boldsymbol{\delta}(\omega t) \quad [22]$$

then the kinematics become:

$$\dot{\overline{\mathbf{p}}}(t) = \overline{\mathbf{R}}(t) \mathbf{V}_\eta(\omega t) \frac{\eta(t)}{\omega} + \overline{\mathbf{R}}(t) \overline{\mathbf{V}} \quad [23]$$

$$\dot{\overline{\mathbf{R}}}(t) = \overline{\mathbf{R}}(t) \widehat{\boldsymbol{\Omega}}_\eta(\omega t) \eta(t) \quad [24]$$

We compute the expressions for $\mathbf{V}_\eta, \boldsymbol{\Omega}_\eta$ which turn out to be:

$$\boldsymbol{\Omega}_\eta(\omega t) = \left(\omega_{\parallel,1} \frac{\omega_{\parallel,0}}{\omega} + \omega_{\perp,1} \frac{\omega_{\perp,0}}{\omega} \right) \mathbf{e}_1 + \left(\omega_{\perp,1} \frac{\omega_{\parallel,0}}{\omega} - \omega_{\parallel,1} \frac{\omega_{\perp,0}}{\omega} \right) \mathbf{e}_3(\omega t) \quad [25]$$

$$\mathbf{V}_\eta(\omega t) = \frac{v\omega_{\perp,0}}{\omega} \left(\omega_{\perp,1} \frac{\omega_{\parallel,0}}{\omega} - \omega_{\parallel,1} \frac{\omega_{\perp,0}}{\omega} \right) \mathbf{e}_1 - \frac{v\omega_{\perp,0}}{\omega} \left(\omega_{\parallel,1} \frac{\omega_{\parallel,0}}{\omega} + \omega_{\perp,1} \frac{\omega_{\perp,0}}{\omega} \right) \mathbf{e}_3(\omega t) \quad [26]$$

Observe that the feedback coefficients $\mathbf{V}_\eta, \boldsymbol{\Omega}_\eta$ are periodic with non zero average in general, whereas the periodic perturbation $\boldsymbol{\delta}(\omega t)$ always has zero average. Let $\varepsilon = \frac{1}{\omega}$, and observe that the instantaneous local concentration $c(\mathbf{p}(t))$ may be approximated by its first order Taylor series:

$$c(\mathbf{p}(t)) = c(\overline{\mathbf{p}}(t) + \varepsilon \overline{\mathbf{R}}(t) \boldsymbol{\delta}(\omega t)) = c(\overline{\mathbf{p}}(t)) + \varepsilon \nabla c(\overline{\mathbf{p}}(t))^\top \overline{\mathbf{R}}(t) \boldsymbol{\delta}(\omega t) + \mathcal{O}(\varepsilon^2) \quad [27]$$

as long as $\|\boldsymbol{\delta}(\omega t)\| \cdot \|\nabla c(\overline{\mathbf{p}}(t))\| = \mathcal{O}(1)$ and $0 < \varepsilon \ll 1$. By employing the fundamental theorem of calculus, the average local concentration $c(\overline{\mathbf{p}}(t))$ can be written as:

$$c(\overline{\mathbf{p}}(t)) = c(\overline{\mathbf{p}}(t)) + \int_t^t \nabla c(\overline{\mathbf{p}}(\tau))^\top \dot{\overline{\mathbf{p}}}(\tau) d\tau = c(\overline{\mathbf{p}}(t)) + \int_t^t \nabla c(\overline{\mathbf{p}}(\tau))^\top \overline{\mathbf{R}}(\tau) (\varepsilon \mathbf{V}_\eta(\omega \tau) \eta(\tau) + \overline{\mathbf{V}}) d\tau \quad [28]$$

Hence, the instantaneous local concentration can be expressed as:

$$c(\mathbf{p}(t)) = c(\overline{\mathbf{p}}(t)) + \int_t^t \nabla c(\overline{\mathbf{p}}(\tau))^\top \overline{\mathbf{R}}(\tau) \overline{\mathbf{V}} d\tau + \varepsilon \nabla c(\overline{\mathbf{p}}(t))^\top \overline{\mathbf{R}}(t) \boldsymbol{\delta}(\omega t) + \varepsilon \int_t^t \nabla c(\overline{\mathbf{p}}(\tau))^\top \overline{\mathbf{R}}(\tau) \mathbf{V}_\eta(\omega \tau) \eta(\tau) d\tau + \mathcal{O}(\varepsilon^2) \quad [29]$$

In the absence of feedback (i.e. when $\eta(t) = 0$), the instantaneous local concentration is given by:

$$c(\mathbf{p}(t)) = c(\overline{\mathbf{p}}(t)) + \int_t^t \nabla c(\overline{\mathbf{p}}(\tau))^\top \overline{\mathbf{R}}(\tau) \overline{\mathbf{V}} d\tau + \varepsilon \nabla c(\overline{\mathbf{p}}(t))^\top \overline{\mathbf{R}}(t) \boldsymbol{\delta}(\omega t) + \mathcal{O}(\varepsilon^2) \quad [30]$$

Over a short time duration $t \leq t' \leq t + \varepsilon$, the integral in the expression for $c(\mathbf{p}(t))$ may be approximated by its first order Taylor series:

$$\int_t^{t'} \nabla c(\overline{\mathbf{p}}(\tau))^\top \overline{\mathbf{R}}(\tau) \overline{\mathbf{V}} d\tau \approx \nabla c(\overline{\mathbf{p}}(t))^\top \overline{\mathbf{R}}(t) \overline{\mathbf{V}} (t' - t) + \mathcal{O}(\varepsilon^2) \approx \varepsilon \nabla c(\overline{\mathbf{p}}(t))^\top \overline{\mathbf{R}}(t) \overline{\mathbf{V}} \omega \Delta t + \mathcal{O}(\varepsilon^2) \quad [31]$$

where $\Delta t = t' - t$. The same applies to the average position $\bar{\mathbf{p}}(t) \approx \bar{\mathbf{p}}(t) + \mathcal{O}(\varepsilon)$ and average orientation $\bar{\mathbf{R}}(t) \approx \bar{\mathbf{R}}(t) + \mathcal{O}(\varepsilon)$. Hence, over an $\mathcal{O}(\varepsilon)$ time duration $t \leq t' \leq t + \varepsilon$, the instantaneous local concentration $c(\mathbf{p}(t))$ can be approximated by:

$$c(\mathbf{p}(t)) = c(\bar{\mathbf{p}}(t)) + \varepsilon \nabla c(\bar{\mathbf{p}}(t))^\top \bar{\mathbf{R}}(t) (\bar{\mathbf{V}} \omega \Delta t + \boldsymbol{\delta}(\omega t)) + \mathcal{O}(\varepsilon^2) \quad [32]$$

A time scale change to $\sigma = \omega \Delta t$ puts the instantaneous local concentration in the form:

$$c(\mathbf{p}(\sigma)) = c(\bar{\mathbf{p}}(t)) + \varepsilon \nabla c(\bar{\mathbf{p}}(t))^\top \bar{\mathbf{R}}(t) (\bar{\mathbf{V}} \sigma + \boldsymbol{\delta}(\sigma)) + \mathcal{O}(\varepsilon^2) \quad [33]$$

The stimulus to which the signaling pathway is exposed due to the binding of the SAP molecules may be taken as:

$$s(t) \approx c(\mathbf{p}(t)) \quad [34]$$

Hence, the approximate form of the stimulus in the time scale σ starting at t is:

$$s(\sigma) \approx c(\bar{\mathbf{p}}(t)) + \varepsilon \|\nabla c(\bar{\mathbf{p}}(t))\| \left(\frac{\nabla c(\bar{\mathbf{p}}(t))^\top}{\|\nabla c(\bar{\mathbf{p}}(t))\|} \bar{\mathbf{R}}(t) \bar{\mathbf{V}} \sigma + \frac{\nabla c(\bar{\mathbf{p}}(t))^\top}{\|\nabla c(\bar{\mathbf{p}}(t))\|} \bar{\mathbf{R}}(t) \boldsymbol{\delta}(\sigma) \right) + \mathcal{O}(\varepsilon^2) \quad [35]$$

Recalling that the triad $\mathbf{e}_1, \mathbf{e}_2(\omega t), \mathbf{e}_3(\omega t)$ forms an orthonormal basis, and that $\mathbf{e}_2(\omega t)$ completes a full rotation in the plane that is orthogonal to \mathbf{e}_1 with frequency ω , one can see that:

$$\frac{\nabla c(\bar{\mathbf{p}}(t))^\top}{\|\nabla c(\bar{\mathbf{p}}(t))\|} \bar{\mathbf{R}}(t) \mathbf{e}_1 = \cos(\theta(t)) \quad [36]$$

$$\frac{\nabla c(\bar{\mathbf{p}}(t))^\top}{\|\nabla c(\bar{\mathbf{p}}(t))\|} \bar{\mathbf{R}}(t) \mathbf{e}_2(\sigma) = \sqrt{1 - \cos(\theta(t))^2} \sin(\sigma + \phi_0(t)) \quad [37]$$

where $\theta(t)$ is the angle between the normalized gradient $\bar{\mathbf{R}}(t)^\top \frac{\nabla c(\bar{\mathbf{p}}(t))}{\|\nabla c(\bar{\mathbf{p}}(t))\|}$ and the vector \mathbf{e}_1 , and the angle $\phi_0(t)$ depends on the initial angle between $\mathbf{e}_2(\sigma)$ and the projection of $\bar{\mathbf{R}}(t)^\top \frac{\nabla c(\bar{\mathbf{p}}(t))}{\|\nabla c(\bar{\mathbf{p}}(t))\|}$ on the plane that is orthogonal to \mathbf{e}_1 . Consequently, the stimulus maybe approximated by:

$$s(\sigma) \approx c(\bar{\mathbf{p}}(t)) + \varepsilon v \|\nabla c(\bar{\mathbf{p}}(t))\| \left(\frac{\omega_{\parallel,0}}{\omega} \cos(\theta(t)) \sigma + \frac{\omega_{\perp,0}}{\omega} \sqrt{1 - \cos(\theta(t))^2} \sin(\sigma + \phi_0(t)) \right) + \mathcal{O}(\varepsilon^2) \quad [38]$$

This form of the input passes through the model of the signaling pathway given in the time scale σ by:

$$\sigma_1 \omega \frac{d\zeta_1}{d\sigma} = \zeta_2(\sigma) - \zeta_1(\sigma) \quad [39]$$

$$\sigma_2 \omega \frac{d\zeta_2}{d\sigma} = s(\sigma) - \zeta_2(\sigma) \quad [40]$$

$$\zeta(\sigma) = \zeta_2(\sigma) - \zeta_1(\sigma) \quad [41]$$

$$\mu \omega \frac{d\rho}{d\sigma} = \rho(\sigma) (1 - (\rho(\sigma) \zeta(\sigma))^2) \quad [42]$$

$$\eta(\sigma) = \rho(\sigma) \zeta(\sigma) \quad [43]$$

The first three equations [39]-[41] are decoupled from the fourth. Moreover, they are linear with a transfer function $G(\lambda)$ given by:

$$G(\lambda) = \mathcal{L} \left\{ \frac{\zeta(t)}{s(t)} \right\} = \frac{\sigma_1 \omega \lambda}{(1 + \sigma_1 \omega \lambda)(1 + \sigma_2 \omega \lambda)} \quad [44]$$

For simplicity, we assume that $\sigma_1 = \sigma_2 = \sigma_c = \mathcal{O}(\varepsilon)$ so that $\sigma_c \omega = \mathcal{O}(1)$ and the transients vanish fast enough without affecting the quasi steady behavior. A direct application of linear analysis techniques yields the following expression for the quasi-steady signal $\zeta(t)$ under the stimulus input given by [38]:

$$\zeta(\sigma) \approx \varepsilon v \sigma_c \omega \|\nabla c(\bar{\mathbf{p}}(t))\| \left(\frac{\omega_{\parallel,0}}{\omega} \cos(\theta(t)) + \frac{v \omega_{\perp,0}}{\omega} \frac{1}{(1 + \omega^2 \sigma_c^2)} \sqrt{1 - \cos(\theta)^2} \sin(\sigma + \phi + \phi_0) \right) \quad [45]$$

where ϕ is the phase contribution of the transfer function $G(\lambda)$, and is such that:

$$\tan(\phi) = \frac{1 - \sigma_c^2 \omega^2}{2 \omega \sigma_c} \quad [46]$$

Next, this quasi steady $\zeta(\sigma)$ is applied as an input to the adaptation equation [42]. We observe that ζ has the form:

$$\zeta(\sigma) = \nu_0 (\nu_1 + \nu_2 \sin(\omega t + \phi + \phi_0)) \quad [47]$$

where the constants ν_1, ν_2 are given by:

$$\nu_0 = \varepsilon v \sigma_c \omega \|\nabla c(\bar{\mathbf{p}}(t))\| > 0, \quad \nu_1 = \frac{\omega_{\parallel,0}}{\omega} \cos(\theta(t)), \quad \nu_2 = \frac{\omega_{\perp,0}}{\omega} \frac{1}{(1 + \omega^2 \sigma_c^2)} \sqrt{1 - \cos(\theta(t))^2} \quad [48]$$

Hence, a quasi steady approximation of equation [42] becomes:

$$\mu\omega \frac{d\rho}{d\sigma} = \rho(\sigma) \left(1 - \nu_0^2 \rho(\sigma)^2 (\nu_1 + \nu_2 \sin(\sigma + \phi + \phi_0))^2\right) \quad [49]$$

This is a first order nonlinear differential equation with periodic coefficients. Fortunately, an exact solution may be obtained and the quasi steady state approximation of the solution is given by the expression:

$$\rho(\sigma) = \frac{1}{\nu_0 \sqrt{\nu_1^2 + \frac{\nu_2^2}{2} - \frac{4\nu_1\nu_2(\mu\omega \cos(\sigma + \phi + \phi_0) - 2 \sin(\sigma + \phi + \phi_0))}{\mu^2\omega^2 + 4} - \frac{\nu_2^2(\mu\omega \sin(2(\sigma + \phi + \phi_0)) + \cos(2(\sigma + \phi + \phi_0)))}{2\mu^2\omega^2 + 2}} \quad [50]$$

Consequently, the quasi steady signal $\eta(\sigma)$ is given by:

$$\eta(\sigma) = \frac{\nu_1 + \nu_2 \sin(\sigma + \phi + \phi_0)}{\sqrt{\nu_1^2 + \frac{\nu_2^2}{2} - \frac{4\nu_1\nu_2(\mu\omega \cos(\sigma + \phi + \phi_0) - 2 \sin(\sigma + \phi + \phi_0))}{\mu^2\omega^2 + 4} - \frac{\nu_2^2(\mu\omega \sin(2(\sigma + \phi + \phi_0)) + \cos(2(\sigma + \phi + \phi_0)))}{2\mu^2\omega^2 + 2}} \quad [51]$$

We observe that the signal $\eta(\sigma)$ is independent of ν_0 (i.e. the magnitude of the gradient). If we make a time variable change to $\tau = \sigma + \phi + \phi_0$ and expand $\eta(t)$ as a Fourier series in τ , we obtain:

$$\eta(\tau) \approx \beta_1(\nu_1, \nu_2) + \beta_2(\nu_1, \nu_2) \sin(\tau) + \beta_3(\nu_1, \nu_2) \cos(\tau) + \text{H.O.H} \quad [52]$$

where the coefficients $\beta_1, \beta_2, \beta_3$ are given by the integrals:

$$\beta_1(\nu_1, \nu_2) = \frac{1}{2\pi} \int_{-\pi}^{\pi} \frac{(\nu_1 + \nu_2 \sin(\tau))}{\sqrt{\nu_1^2 + \frac{\nu_2^2}{2} - \frac{4\nu_1\nu_2(\mu\omega \cos(\tau) - 2 \sin(\tau))}{\mu^2\omega^2 + 4} - \frac{\nu_2^2(\mu\omega \sin(2\tau) + \cos(2\tau))}{2\mu^2\omega^2 + 2}} d\tau \quad [53]$$

$$\beta_2(\nu_1, \nu_2) = \frac{1}{\pi} \int_{-\pi}^{\pi} \frac{(\nu_1 + \nu_2 \sin(\tau)) \sin(\tau)}{\sqrt{\nu_1^2 + \frac{\nu_2^2}{2} - \frac{4\nu_1\nu_2(\mu\omega \cos(\tau) - 2 \sin(\tau))}{\mu^2\omega^2 + 4} - \frac{\nu_2^2(\mu\omega \sin(2\tau) + \cos(2\tau))}{2\mu^2\omega^2 + 2}} d\tau \quad [54]$$

$$\beta_3(\nu_1, \nu_2) = \frac{1}{\pi} \int_{-\pi}^{\pi} \frac{(\nu_1 + \nu_2 \sin(\tau)) \cos(\tau)}{\sqrt{\nu_1^2 + \frac{\nu_2^2}{2} - \frac{4\nu_1\nu_2(\mu\omega \cos(\tau) - 2 \sin(\tau))}{\mu^2\omega^2 + 4} - \frac{\nu_2^2(\mu\omega \sin(2\tau) + \cos(2\tau))}{2\mu^2\omega^2 + 2}} d\tau \quad [55]$$

In the case when $\mu\omega = \mathcal{O}(\varepsilon)$, a singular perturbation calculation leads to the quasi steady approximation:

$$\eta(\sigma) \approx \text{sign}(\nu_1 + \nu_2 \sin(\sigma + \phi + \phi_0)) + \mathcal{O}(\varepsilon) \quad [56]$$

for which the coefficients $\beta_1(\nu_1, \nu_2), \beta_2(\nu_1, \nu_2), \beta_3(\nu_1, \nu_2)$ become:

$$\beta_1(\nu_1, \nu_2) = \begin{cases} \text{sign}(\nu_1) & |\nu_1| \geq |\nu_2| \\ \frac{2}{\pi} \text{sign}(\nu_1) \arcsin\left(\left|\frac{\nu_1}{\nu_2}\right|\right) & |\nu_1| < |\nu_2| \end{cases}, \quad \beta_2(\nu_1, \nu_2) = \begin{cases} 0 & |\nu_1| \geq |\nu_2| \\ \frac{4}{\pi} \text{sign}(\nu_2) \sqrt{1 - \left|\frac{\nu_1}{\nu_2}\right|^2} & |\nu_1| < |\nu_2| \end{cases}, \quad \beta_3(\nu_1, \nu_2) = 0$$

One can see that the gains β_1, β_2 satisfy the relation:

$$\beta_1(\nu_1, \nu_2)^2 + \beta_2(\nu_1, \nu_2)^2 = \begin{cases} 1 & |\nu_1| \geq |\nu_2| \\ \frac{4}{\pi^2} \arcsin\left(\left|\frac{\nu_1}{\nu_2}\right|\right)^2 + \frac{16}{\pi^2} \left(1 - \left|\frac{\nu_1}{\nu_2}\right|^2\right) & |\nu_1| < |\nu_2| \end{cases} \quad [57]$$

from which it is easy to see that $\beta_1(\nu_1, \nu_2), \beta_2(\nu_1, \nu_2)$ satisfy the inequality:

$$1 \leq \beta_1(\nu_1, \nu_2)^2 + \beta_2(\nu_1, \nu_2)^2 \leq \frac{16}{\pi^2} \approx 1.62 \quad [58]$$

as long as $\nu_1^2 + \nu_2^2 \neq 0$. Let us define the gains ρ_1 and ρ_2 by:

$$\rho_1 = \left| \frac{\beta_1(\nu_1, \nu_2)}{v\nu_1} \right|, \quad \rho_2 = \left| \frac{\beta_2(\nu_1, \nu_2)}{v\nu_2} \right| \quad [59]$$

and observe that under this definition, the gains $\beta_1(\nu_1, \nu_2)$ and $\beta_2(\nu_1, \nu_2)$ can now be written as:

$$\beta_1(\nu_1, \nu_2) = \rho_1(\nu_1, \nu_2) \nu_1 v, \quad \beta_2(\nu_1, \nu_2) = \rho_2(\nu_1, \nu_2) \nu_2 v \quad [60]$$

which implies that the quasi steady approximation of $\eta(\tau)$ is now:

$$\eta(\tau) \approx v\rho_1(\nu_1, \nu_2)\nu_1 + v\rho_2(\nu_1, \nu_2)\nu_2 \sin(\tau) \quad \Longrightarrow \quad \eta(t) \approx v\rho_1\nu_1 + v\rho_2\nu_2 \sin(\omega t + \phi + \phi_0) \quad [61]$$

Recalling equation [38] and [48] and the definition of τ , one can see that in the original time variable t , the signal $\eta(t)$ can be approximated in the quasi steady sense by:

$$\eta(t) \approx (\rho_1\bar{\mathbf{V}} + \rho_2\delta(\omega t + \phi))^\top \bar{\mathbf{R}}(t)^\top \frac{\nabla c(\bar{\mathbf{p}}(t))}{\|\nabla c(\bar{\mathbf{p}}(t))\|} \quad [62]$$

Using this expression for $\eta(t)$, the kinematics become:

$$\dot{\bar{\mathbf{p}}}(t) = \bar{\mathbf{R}}(t)\mathbf{V}_\eta(\omega t)\eta(t)\varepsilon + \bar{\mathbf{R}}(t)\bar{\mathbf{V}} \quad [63]$$

$$\dot{\bar{\mathbf{R}}}(t) = \bar{\mathbf{R}}(t)\hat{\boldsymbol{\Omega}}_\eta(\omega t)\eta(t) \quad [64]$$

where the feedback terms $\mathbf{V}_\eta(\omega t)\eta(t)$ and $\boldsymbol{\Omega}_\eta(\omega t)\eta(t)$ are given by:

$$\mathbf{V}_\eta(\omega t)\eta(t) = \mathbf{M}_1(\omega t)\bar{\mathbf{R}}(t)^\top \frac{\nabla c(\bar{\mathbf{p}}(t))}{\|\nabla c(\bar{\mathbf{p}}(t))\|} \quad [65]$$

$$\boldsymbol{\Omega}_\eta(\omega t)\eta(t) = \mathbf{M}_2(\omega t)\bar{\mathbf{R}}(t)^\top \frac{\nabla c(\bar{\mathbf{p}}(t))}{\|\nabla c(\bar{\mathbf{p}}(t))\|} \quad [66]$$

and the matrices \mathbf{M}_1 and \mathbf{M}_2 are given by:

$$\mathbf{M}_1(\omega t) = \left(\left(\omega_{\perp,1} \frac{\omega_{\parallel,0}}{\omega} - \omega_{\parallel,1} \frac{\omega_{\perp,0}}{\omega} \right) \mathbf{e}_1 - \left(\omega_{\parallel,1} \frac{\omega_{\parallel,0}}{\omega} + \omega_{\perp,1} \frac{\omega_{\perp,0}}{\omega} \right) \mathbf{e}_3(\omega t) \right) (\rho_1\bar{\mathbf{V}} + \rho_2\delta(\omega t + \phi))^\top \quad [67]$$

$$\mathbf{M}_2(\omega t) = \left(\left(\omega_{\parallel,1} \frac{\omega_{\parallel,0}}{\omega} + \omega_{\perp,1} \frac{\omega_{\perp,0}}{\omega} \right) \mathbf{e}_1 + \left(\omega_{\perp,1} \frac{\omega_{\parallel,0}}{\omega} - \omega_{\parallel,1} \frac{\omega_{\perp,0}}{\omega} \right) \mathbf{e}_3(\omega t) \right) (\rho_1\bar{\mathbf{V}} + \rho_2\delta(\omega t + \phi))^\top \quad [68]$$

Observe that

$$\delta(\omega t + \phi) = \frac{v\omega_{\perp,0}}{\omega} \mathbf{e}_2(\omega t + \phi) = \frac{v\omega_{\perp,0}}{\omega} \begin{pmatrix} \frac{\omega_{\perp,0}}{\omega} \sin(\omega t + \phi) \\ -\cos(\omega t + \phi) \\ -\frac{\omega_{\parallel,0}}{\omega} \sin(\omega t + \phi) \end{pmatrix} = \frac{v\omega_{\perp,0}}{\omega} \cos(\phi) \mathbf{e}_2(\omega t) + \frac{v\omega_{\perp,0}}{\omega} \sin(\phi) \mathbf{e}_3(\omega t) \quad [69]$$

Thus, we have:

$$\mathbf{M}_1(\omega t) = \left(\frac{\omega_{\perp,1}\omega_{\parallel,0} - \omega_{\parallel,1}\omega_{\perp,0}}{\omega} \right) \left(\frac{v\rho_1\omega_{\parallel,0}}{\omega} \mathbf{e}_1 \mathbf{e}_1^\top + \frac{v\rho_2\omega_{\perp,0}}{\omega} (\cos(\phi) \mathbf{e}_1 \mathbf{e}_2(\omega t)^\top + \sin(\phi) \mathbf{e}_1 \mathbf{e}_3(\omega t)^\top) \right) \quad [70]$$

$$- \left(\frac{\omega_{\parallel,1}\omega_{\parallel,0} + \omega_{\perp,1}\omega_{\perp,0}}{\omega} \right) \left(\frac{v\rho_1\omega_{\parallel,0}}{\omega} \mathbf{e}_3(\omega t) \mathbf{e}_1^\top + \frac{v\rho_2\omega_{\perp,0}}{\omega} (\cos(\phi) \mathbf{e}_3(\omega t) \mathbf{e}_2(\omega t)^\top + \sin(\phi) \mathbf{e}_3(\omega t) \mathbf{e}_3(\omega t)^\top) \right) \quad [71]$$

$$\mathbf{M}_2(\omega t) = \left(\frac{\omega_{\parallel,1}\omega_{\parallel,0} + \omega_{\perp,1}\omega_{\perp,0}}{\omega} \right) \left(\frac{v\rho_1\omega_{\parallel,0}}{\omega} \mathbf{e}_1 \mathbf{e}_1^\top + \frac{v\rho_2\omega_{\perp,0}}{\omega} (\cos(\phi) \mathbf{e}_1 \mathbf{e}_2(\omega t)^\top + \sin(\phi) \mathbf{e}_1 \mathbf{e}_3(\omega t)^\top) \right) \quad [72]$$

$$+ \left(\frac{\omega_{\perp,1}\omega_{\parallel,0} - \omega_{\parallel,1}\omega_{\perp,0}}{\omega} \right) \left(\frac{v\rho_1\omega_{\parallel,0}}{\omega} \mathbf{e}_3(\omega t) \mathbf{e}_1^\top + \frac{v\rho_2\omega_{\perp,0}}{\omega} (\cos(\phi) \mathbf{e}_3(\omega t) \mathbf{e}_2(\omega t)^\top + \sin(\phi) \mathbf{e}_3(\omega t) \mathbf{e}_3(\omega t)^\top) \right) \quad [73]$$

If we change to the time scale $\sigma = \omega t$, then the equations become:

$$\frac{d\bar{\mathbf{p}}}{d\sigma} = \varepsilon \bar{\mathbf{R}}(\sigma) \bar{\mathbf{V}} + \varepsilon^2 \bar{\mathbf{R}}(\sigma) \mathbf{V}_\eta(\sigma) \eta(\sigma) \quad [74]$$

$$\frac{d\bar{\mathbf{R}}}{d\sigma} = \varepsilon \bar{\mathbf{R}}(\sigma) \hat{\boldsymbol{\Omega}}_\eta(\sigma) \eta(\sigma) \quad [75]$$

which is on the canonical averaging form. Before we proceed, we compute some important time averages that will come up when we attempt to apply the averaging theorem:

$$\overline{\mathbf{e}_1 \mathbf{e}_2(\sigma)^\top} = 0, \quad \overline{\mathbf{e}_2(\sigma) \mathbf{e}_2(\sigma)^\top} = \frac{1}{2} (\mathbf{I} - \mathbf{e}_1 \mathbf{e}_1^\top), \quad \overline{\mathbf{e}_2(\sigma) \mathbf{e}_3(\sigma)^\top} = -\frac{1}{2} \hat{\mathbf{e}}_1 \quad [76]$$

$$\overline{\mathbf{e}_1 \mathbf{e}_3(\sigma)^\top} = 0, \quad \overline{\mathbf{e}_3(\sigma) \mathbf{e}_3(\sigma)^\top} = \frac{1}{2} (\mathbf{I} - \mathbf{e}_1 \mathbf{e}_1^\top), \quad \overline{\mathbf{e}_3(\sigma) \mathbf{e}_2(\sigma)^\top} = \frac{1}{2} \hat{\mathbf{e}}_1 \quad [77]$$

2D Chemotaxis. When the motion is confined to a plane, we will have that $\omega_{\parallel,0} = \omega_{\parallel,1} = \rho_1 = 0$, which greatly simplifies the expressions for the system. In particular, in the 2D case we will have:

$$\mathbf{M}_1(\sigma) = -v\rho_2\omega_{\perp,1}\text{sign}(\omega_{\perp,0}) (\cos(\phi)\mathbf{e}_3(\sigma)\mathbf{e}_2(\sigma)^\top + \sin(\phi)\mathbf{e}_3(\sigma)\mathbf{e}_3(\sigma)^\top) \quad [78]$$

$$\mathbf{M}_2(\sigma) = 0 \quad [79]$$

which leads to:

$$\frac{d\bar{\mathbf{p}}}{d\sigma} = \varepsilon^2 \bar{\mathbf{R}}(\sigma) \mathbf{M}_1(\sigma) \bar{\mathbf{R}}(\sigma)^\top \frac{\nabla c(\bar{\mathbf{p}}(\sigma))}{\|\nabla c(\bar{\mathbf{p}}(\sigma))\|} \quad [80]$$

$$\frac{d\bar{\mathbf{R}}}{d\sigma} = 0 \quad [81]$$

Moreover, the vector \mathbf{e}_1 will be:

$$\mathbf{e}_1 = \begin{pmatrix} 0 \\ 0 \\ 1 \end{pmatrix} \quad [82]$$

By applying the averaging theorem to second order in ε , we obtain the system:

$$\frac{d\bar{\mathbf{p}}}{d\sigma} = \varepsilon^2 \bar{\mathbf{R}}(\sigma) \overline{\mathbf{M}_1(\sigma)} \bar{\mathbf{R}}(\sigma)^\top \frac{\nabla c(\bar{\mathbf{p}}(\sigma))}{\|\nabla c(\bar{\mathbf{p}}(\sigma))\|} \quad [83]$$

$$\frac{d\bar{\mathbf{R}}}{d\sigma} = 0 \quad [84]$$

where $\overline{\mathbf{M}_1(\sigma)}$ is the time average of $\mathbf{M}_1(\sigma)$. Now, we compute:

$$\overline{\mathbf{M}_1(\sigma)} = -v\rho_2\omega_{\perp,1}\text{sign}(\omega_{\perp,0}) (\cos(\phi)\overline{\mathbf{e}_3(\sigma)\mathbf{e}_2(\sigma)^\top} + \sin(\phi)\overline{\mathbf{e}_3(\sigma)\mathbf{e}_3(\sigma)^\top}) = -\frac{v\rho_2\omega_{\perp,1}}{2} (\cos(\phi)\hat{\mathbf{e}}_1 + \sin(\phi)(\mathbf{I} - \mathbf{e}_1\mathbf{e}_1^\top)) \quad [85]$$

Consequently, we obtain that the average local concentration evolves according to the differential equation:

$$\frac{d}{d\sigma} (c(\bar{\mathbf{p}}(\sigma))) = \nabla c(\bar{\mathbf{p}}(\sigma))^\top \frac{d\bar{\mathbf{p}}}{d\sigma} = \varepsilon^2 \nabla c(\bar{\mathbf{p}}(\sigma))^\top \bar{\mathbf{R}}(\sigma) \overline{\mathbf{M}_1(\sigma)} \bar{\mathbf{R}}(\sigma)^\top \frac{\nabla c(\bar{\mathbf{p}}(\sigma))}{\|\nabla c(\bar{\mathbf{p}}(\sigma))\|} \quad [86]$$

Since the motion is confined to a plane, we may assume, without loss of generality, that $\mathbf{e}_1^\top \bar{\mathbf{R}}(\sigma)^\top \nabla c(\bar{\mathbf{p}}(\sigma)) = 0$, which leads to:

$$\frac{d}{d\sigma} (c(\bar{\mathbf{p}}(\sigma))) = -\frac{v\rho_2\omega_{\perp,1}}{2} \text{sign}(\omega_{\perp,0}) \varepsilon^2 \nabla c(\bar{\mathbf{p}}(\sigma))^\top \bar{\mathbf{R}}(\sigma) (\cos(\phi)\hat{\mathbf{e}}_1 + \sin(\phi)\mathbf{I}) \bar{\mathbf{R}}(\sigma)^\top \frac{\nabla c(\bar{\mathbf{p}}(\sigma))}{\|\nabla c(\bar{\mathbf{p}}(\sigma))\|} \quad [87]$$

$$= -\frac{v\rho_2\omega_{\perp,1}}{2} \text{sign}(\omega_{\perp,0}) \varepsilon^2 \sin(\phi) \|\nabla c(\bar{\mathbf{p}}(\sigma))\| \quad [88]$$

Going back to the time scale $t = \varepsilon\sigma$, we obtain the equation:

$$\frac{d}{dt} (c(\bar{\mathbf{p}}(t))) = -\frac{v\rho_2\omega_{\perp,1}}{2} \text{sign}(\omega_{\perp,0}) \varepsilon \sin(\phi) \|\nabla c(\bar{\mathbf{p}}(t))\| \quad [89]$$

Define the constant $\gamma = \frac{v\rho_2\varepsilon}{2|\omega_{\perp,0}|}$, and observe that the equation becomes:

$$\frac{d}{dt} (c(\bar{\mathbf{p}}(t))) = -\gamma \omega_{\perp,0} \omega_{\perp,1} \sin(\phi) \|\nabla c(\bar{\mathbf{p}}(t))\| \quad [90]$$

2 For successful 2D chemotaxis, it is required that $\omega_{\perp,0} \omega_{\perp,1} \sin(\phi) < 0$.

3D Chemotaxis. In the 3D case, the leading order behavior is the first order in $\mathcal{O}(\varepsilon)$. Hence, we compute only first order averaging:

$$\frac{d\bar{\mathbf{p}}}{d\sigma} = \varepsilon \bar{\mathbf{R}}(\sigma) \bar{\mathbf{V}} \quad [91]$$

$$\frac{d\bar{\mathbf{R}}}{d\sigma} = \varepsilon \bar{\mathbf{R}}(\sigma) \widehat{\overline{\mathbf{\Omega}_\eta(\sigma)\eta(\sigma)}} \quad [92]$$

where:

$$\widehat{\overline{\mathbf{\Omega}_\eta(\sigma)\eta(\sigma)}} = \overline{\mathbf{M}_2(\sigma)} \bar{\mathbf{R}}(\sigma)^\top \frac{\nabla c(\bar{\mathbf{p}}(\sigma))}{\|\nabla c(\bar{\mathbf{p}}(\sigma))\|} \quad [93]$$

We proceed with the averaging computation:

$$\overline{\mathbf{M}_2(\sigma)} = \frac{v\rho_1\omega_{\parallel,0}}{\omega} \left(\frac{\omega_{\parallel,1}\omega_{\parallel,0} + \omega_{\perp,1}\omega_{\perp,0}}{\omega} \right) \mathbf{e}_1 \mathbf{e}_1^\top + \frac{v\rho_2\omega_{\perp,0}}{2\omega} \left(\frac{\omega_{\perp,1}\omega_{\parallel,0} - \omega_{\parallel,1}\omega_{\perp,0}}{\omega} \right) (\cos(\phi)\widehat{\mathbf{e}}_1 + \sin(\phi)(\mathbf{I} - \mathbf{e}_1 \mathbf{e}_1^\top)) \quad [94]$$

If we define the unit vector $\bar{\mathbf{q}}(\sigma) = \overline{\mathbf{R}}(\sigma)\mathbf{e}_1$, we obtain that:

$$\frac{d\bar{\mathbf{q}}}{d\sigma} = \frac{d\overline{\mathbf{R}}}{d\sigma} \mathbf{e}_1 = \varepsilon \overline{\mathbf{R}}(\sigma) \widehat{\overline{\boldsymbol{\Omega}}_\eta(\sigma)\eta(\sigma)} \mathbf{e}_1 = \varepsilon \overline{\mathbf{R}}(\sigma) (\overline{\boldsymbol{\Omega}}_\eta(\sigma)\eta(\sigma) \times \mathbf{e}_1) = -\varepsilon \overline{\mathbf{R}}(\sigma) \widehat{\mathbf{e}}_1 \overline{\boldsymbol{\Omega}}_\eta(\sigma)\eta(\sigma) \quad [95]$$

$$= -\varepsilon \overline{\mathbf{R}}(\sigma) \widehat{\mathbf{e}}_1 \overline{\mathbf{M}_2(\sigma)} \overline{\mathbf{R}}(\sigma)^\top \frac{\nabla c(\bar{\mathbf{p}}(\sigma))}{\|\nabla c(\bar{\mathbf{p}}(\sigma))\|} \quad [96]$$

We compute:

$$\widehat{\mathbf{e}}_1 \overline{\mathbf{M}_2(\sigma)} = \frac{v\rho_2\omega_{\perp,0}}{2\omega} \left(\frac{\omega_{\perp,1}\omega_{\parallel,0} - \omega_{\parallel,1}\omega_{\perp,0}}{\omega} \right) (\cos(\phi)\widehat{\mathbf{e}}_1^2 + \sin(\phi)\widehat{\mathbf{e}}_1) \quad [97]$$

$$= \frac{v\rho_2\omega_{\perp,0}}{2\omega} \left(\frac{\omega_{\perp,1}\omega_{\parallel,0} - \omega_{\parallel,1}\omega_{\perp,0}}{\omega} \right) (\cos(\phi)(\mathbf{e}_1 \mathbf{e}_1^\top - \mathbf{I}) + \sin(\phi)\widehat{\mathbf{e}}_1) \quad [98]$$

Thus, we have:

$$\frac{d\bar{\mathbf{q}}}{d\sigma} = -\varepsilon \frac{v\rho_2\omega_{\perp,0}}{2\omega} \left(\frac{\omega_{\perp,1}\omega_{\parallel,0} - \omega_{\parallel,1}\omega_{\perp,0}}{\omega} \right) \overline{\mathbf{R}}(\sigma) (\cos(\phi)(\mathbf{e}_1 \mathbf{e}_1^\top - \mathbf{I}) + \sin(\phi)\widehat{\mathbf{e}}_1) \overline{\mathbf{R}}(\sigma)^\top \frac{\nabla c(\bar{\mathbf{p}}(\sigma))}{\|\nabla c(\bar{\mathbf{p}}(\sigma))\|} \quad [99]$$

$$= -\varepsilon \frac{v\rho_2\omega_{\perp,0}}{2\omega} \left(\frac{\omega_{\perp,1}\omega_{\parallel,0} - \omega_{\parallel,1}\omega_{\perp,0}}{\omega} \right) (\cos(\phi)(\overline{\mathbf{R}}(\sigma)\mathbf{e}_1 \mathbf{e}_1^\top \overline{\mathbf{R}}(\sigma)^\top - \mathbf{I}) + \sin(\phi)\overline{\mathbf{R}}(\sigma)\widehat{\mathbf{e}}_1 \overline{\mathbf{R}}(\sigma)^\top) \frac{\nabla c(\bar{\mathbf{p}}(\sigma))}{\|\nabla c(\bar{\mathbf{p}}(\sigma))\|} \quad [100]$$

$$= -\varepsilon \frac{v\rho_2\omega_{\perp,0}}{2\omega} \left(\frac{\omega_{\perp,1}\omega_{\parallel,0} - \omega_{\parallel,1}\omega_{\perp,0}}{\omega} \right) (\cos(\phi)(\bar{\mathbf{q}}(\sigma)\bar{\mathbf{q}}(\sigma)^\top - \mathbf{I}) + \sin(\phi)\widehat{\bar{\mathbf{q}}}(\sigma)) \frac{\nabla c(\bar{\mathbf{p}}(\sigma))}{\|\nabla c(\bar{\mathbf{p}}(\sigma))\|} \quad [101]$$

$$= -\varepsilon \frac{v\rho_2\omega_{\perp,0}}{2\omega} \left(\frac{\omega_{\parallel,1}\omega_{\perp,0} - \omega_{\perp,1}\omega_{\parallel,0}}{\omega} \right) \left(\cos(\phi)(\mathbf{I} - \bar{\mathbf{q}}(\sigma)\bar{\mathbf{q}}(\sigma)^\top) \frac{\nabla c(\bar{\mathbf{p}}(\sigma))}{\|\nabla c(\bar{\mathbf{p}}(\sigma))\|} - \sin(\phi)\bar{\mathbf{q}}(\sigma) \times \frac{\nabla c(\bar{\mathbf{p}}(\sigma))}{\|\nabla c(\bar{\mathbf{p}}(\sigma))\|} \right) \quad [102]$$

Recalling the definition of $\bar{\mathbf{q}}$ and $\bar{\mathbf{V}}$, we see that:

$$\frac{d\bar{\mathbf{p}}}{dt} = \frac{v\omega_{\perp,0}}{\omega} \bar{\mathbf{q}} \quad \implies \quad \left\| \frac{d\bar{\mathbf{p}}}{dt} \right\|^2 = \frac{v^2\omega_{\perp,0}^2}{\omega^2} \quad \& \quad \frac{d^2\bar{\mathbf{p}}}{dt^2} = \frac{v\omega_{\perp,0}}{\omega} \frac{d\bar{\mathbf{q}}}{dt} \quad [103]$$

and also that:

$$\bar{\mathbf{q}}(t)\bar{\mathbf{q}}(t)^\top = \frac{\omega^2}{v^2\omega_{\perp,0}^2} \frac{d\bar{\mathbf{p}}}{dt} \frac{d\bar{\mathbf{p}}}{dt}^\top = \left\| \frac{d\bar{\mathbf{p}}}{dt} \right\|^{-2} \frac{d\bar{\mathbf{p}}}{dt} \frac{d\bar{\mathbf{p}}}{dt}^\top \quad [104]$$

Hence, by going back to the time scale $t = \varepsilon\sigma$ we will have:

$$\frac{d^2\bar{\mathbf{p}}}{dt^2} = \gamma_1 \left(\mathbf{I} - \left\| \frac{d\bar{\mathbf{p}}}{dt} \right\|^{-2} \frac{d\bar{\mathbf{p}}}{dt} \frac{d\bar{\mathbf{p}}}{dt}^\top \right) \frac{\nabla c(\bar{\mathbf{p}}(t))}{\|\nabla c(\bar{\mathbf{p}}(t))\|} + \gamma_2 \frac{d\bar{\mathbf{p}}}{dt} \times \frac{\nabla c(\bar{\mathbf{p}}(t))}{\|\nabla c(\bar{\mathbf{p}}(t))\|} \quad [105]$$

where γ_1 and γ_2 are given by:

$$\gamma_1 = -\frac{\rho_2}{2} \frac{v^2\omega_{\perp,0}^2}{\omega^2} \left(\frac{\omega_{\parallel,1}\omega_{\perp,0} - \omega_{\perp,1}\omega_{\parallel,0}}{\omega} \right) \cos(\phi), \quad \gamma_2 = -\frac{\rho_2}{2} \frac{v^2\omega_{\perp,0}^2}{\omega^2} \left(\frac{\omega_{\parallel,1}\omega_{\perp,0} - \omega_{\perp,1}\omega_{\parallel,0}}{\omega} \right) \sin(\phi) \quad [106]$$

When the concentration field is linear: $c(\mathbf{p}) = c_0 + \mathbf{c}_1^\top \mathbf{p}$, a sufficient condition for successful positive chemotaxis is that $\mathbf{c}_1^\top \frac{d\bar{\mathbf{p}}}{dt} > 0$. If we show that $\frac{d}{dt} (\mathbf{c}_1^\top \frac{d\bar{\mathbf{p}}}{dt}) > 0$ when $\mathbf{c}_1^\top \frac{d\bar{\mathbf{p}}}{dt} < K$ for some positive nonzero constant K , then this means that $\mathbf{c}_1^\top \frac{d\bar{\mathbf{p}}}{dt}$ is monotonically increasing which implies that eventually it will become positive. We proceed by the computation:

$$\frac{d}{dt} \left(\mathbf{c}_1^\top \frac{d\bar{\mathbf{p}}}{dt} \right) = \mathbf{c}_1^\top \frac{d^2\bar{\mathbf{p}}}{dt^2} = \gamma_1 \mathbf{c}_1^\top \left(\mathbf{I} - \left\| \frac{d\bar{\mathbf{p}}}{dt} \right\|^{-2} \frac{d\bar{\mathbf{p}}}{dt} \frac{d\bar{\mathbf{p}}}{dt}^\top \right) \frac{\mathbf{c}_1}{\|\mathbf{c}_1\|} = \gamma_1 \|\mathbf{c}_1\| \left(1 - \|\mathbf{c}_1\|^{-2} \left\| \frac{d\bar{\mathbf{p}}}{dt} \right\|^2 \left(\mathbf{c}_1^\top \frac{d\bar{\mathbf{p}}}{dt} \right)^2 \right) \quad [107]$$

It is not hard to see that this quantity is positive as long as $\mathbf{c}_1^\top \frac{d\bar{\mathbf{p}}}{dt} < \|\mathbf{c}_1\| \left\| \frac{d\bar{\mathbf{p}}}{dt} \right\|$ and $\gamma_1 > 0$. Thus, successful positive chemotaxis requires that

$$\gamma_1 > 0 \implies (\omega_{\parallel,1}\omega_{\perp,0} - \omega_{\perp,1}\omega_{\parallel,0}) \cos(\phi) < 0 \quad [108]$$